Lagrangian statistics of turbulence: Some experimental results

Jacob Sparre Andersen*

CATS, Niels Bohr Institute, Blegdamsvej 17,

DK-2100 Copenhagen Ø, Denmark†

Søren Ott and Jakob Mann

Risø National Laboratory, P.O. 49, DK-4000 Roskilde, Denmark

(Dated: 28th August 2002)

Abstract

We present Lagrangian statistics from particle tracking measurements in an experiment with turbulence forced by oscillating grids. Lagrangian acceleration auto-correlation functions and their zero-crossing times are discussed. The zero-crossing time for the Lagrangian acceleration auto-correlation function is not in accordance with Yeung and Pope's suggestion [1] based on their computer simulations. Second order Lagrangian velocity structure functions and the convergence of their maxima to a universal constant are discussed. These results do match Yeung and Pope's computer simulations, as well as Sawford's stochastic model [2].

When we look at turbulence through statistical measures, we typically follow the ideas introduced by Richardson [3] and Kolmogorov [4], and look at the relative motion of different parts of the fluid *at the same time*. In this paper, we will instead follow the example of Taylor [5], Sawford [2], Yeung [6], Pope [7] and others [8–10], and study Lagrangian statistics, i.e. look at the local properties of a turbulent fluid as seen from a particle that follows the flow. It is our ambition to compare experimental data to predictions for Lagrangian acceleration variances, acceleration correlations and velocity structure functions.

The simplicity of the Navier-Stokes equations written in Lagrangian coordinates, makes measurements, which allow a more direct comparison with theoretical work based on Lagrangian formulation, interesting compared with the typical fixed-point measurements made with hot-wire anemometers.

EXPERIMENTAL SETUP

The experimental setup [11, 12] is centered on a $320 \times 320 \times 450$ mm^3 water tank with two transparent walls and a transparent bottom.

Turbulence is induced in fresh water by two vertically oscillating square grids mounted approximately 300 mm apart. Each grid is mounted on four rods and powered by hydraulics. The grid constant is 40 mm and the rods are 8 mm wide. The amplitude of the oscillation of the grids is 25 mm and the data presented here includes forcing by both co-oscillating (runs 20, 21 and 21) and counter-oscillating grids (runs 15, 16 and 17).

The forcing through vertically oscillating grids means that there is a small anisotropy in the system. In terms of the relative values of different components of a_0, the anisotropy is 1.2 in the present experiment, while it for similar values of R_λ is 1.5 in [13].

Tracking particles of neutral buoyancy were produced by boiling industrial grade polystyrene beads [22] of 0.5 mm diameter. We have observed that there is no visible separation into lighter and heavier particles, when we leave them floating in still water for half an hour.

The particles are tracked with four synchronized video cameras observing the same central volume in the water tank from four different angles. The observed volume measures approximately $120 \times 120 \times 150$ mm^3 and it typically contains around 400 particles. The shutter time of the cameras is set such that both half-frames of the images can be recorded at the

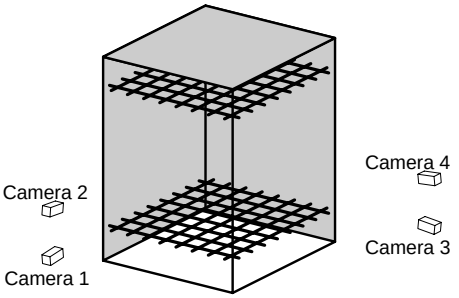

Figure 1: The arrangement of the water tank, the grids and the cameras.

same time, and the particles are illuminated with a 25 Hz stroboscope. The cameras send standard gray-scale PAL signals to a digital video recording system. The recorded movies are then used to reconstruct the particle positions. Particle tracks are created by "joining" particle positions close to each other at subsequent time-steps in a way, that minimises particle acceleration [14, 15].

Velocities and accelerations are derived from the particle tracks. For each measured point on the particle tracks a symmetric window including at least one measurement before, as well as one after, the point of interest is chosen. A polynomium is fitted to these points, and we use its first and second derivatives as estimates of velocity and acceleration of the fluid at the point of interest.

The number of points needed to estimate the velocity and acceleration of a particle is controlled by three things:

- Instantaneous velocities and accelerations are defined as temporal *derivatives*, that is, as limit values for time differences going to zero. Since we are making measurements at a fixed finite frequency this can only be done approximatively, but it means that we should choose the shortest possible time interval – all else being equal.

- The *Kolmogorov time-scale*, τ_η, denotes the lower limit of the time-scales at which turbulenct motion dominates over viscosity, so it has until recently [13] been considered reasonable to fit a low-order polynomium to a number of measured particle positions equivalent to one Kolmogorov time-scale.

- The more points we fit the polynomia to, the less influence have errors in the individual positions measurements on the estimated velocities and accelerations.

Run	R_λ	ϵ	σ	L_{int}	τ_η	η	$f_{forcing}$	$\tau zero$	N
		[mm^2/s^3]	[mm/s]	[mm]	[s]	[mm]	[Hz]	[τ_η]	[10^3]
15	95	108	16	43	0.091	0.28	2.96	1.5	767
16	93	126	16	40	0.084	0.27	2.97	1.4	739
17	84	49	12	43	0.135	0.35	2.00	1.4	800
20	106	234	20	41	0.062	0.23	3.50	1.8	566
21	97	186	18	38	0.069	0.25	3.45	1.6	585
22	80	50	12	40	0.133	0.34	2.00	1.4	639

Table I: The basic flow parameters for the six data-sets included in this article.

The shortest possible time interval we can use to estimate velocities and accelerations is 80 ms. Experiments with Kolmogorov time-scales significantly below 80 ms should therefore be viewed upon with caution. This indicates that using three points, covering an interval of 80 ms, is the best choice with the experimental setup described above, and this choice has thus been used for all the following calculations.

Table I contains a summary of our measurements of the parameters we use to describe turbulent flow, the Taylor micro-scale Reynolds number, R_λ, the average energy dissipation, ϵ, the velocity standard deviation, σ, the integral length-scale, $L_{\mathtt{int}}$, the Kolmogorov time-scale, τ_η, and the Kolmogorov length-scale, η.

The average energy dissipation, ϵ, is calculated by fitting the structure function corresponding to the von Kármán spectrum [12, 16] to the second order Eulerian velocity structure function, assuming that the Kolmogorov constant, C_K, has a value of 2.0. The exact value of C_K is not all that well determined with experimental results in the whole range from 1.75 to 2.75 [17, 18]. The integral length-scale, $L_{\mathtt{int}}$, is defined as the integral of the function $R_{||}(r) = \sigma^2 - \frac{1}{2}\langle \delta v_{||}^2(r) \rangle$. However, we find it through the above mentioned fit of the von Kármán spectrum. The Kolmogorov time-scale is defined as $\tau_\eta = (\frac{\nu}{\epsilon})^{\frac{1}{2}}$ and the Kolmogorov length-scale is defined as $\eta = (\frac{\nu^3}{\epsilon})^{\frac{1}{4}}$. N is the total number of velocity and acceleration measurements in each run of the experiments. The various averages presented in the article have all been made based on all of these measurements. The effective number of statistically independent data points is thus $2\tau_\eta/40$ ms times lower than N. A detailed discussion of the derivation of the basic flow parameters, as well as a more detailed description of the

experiment, can be found in [11, 12].

ACCELERATION VARIANCE

The large number of particle tracks collected in these measurements give us a unique possibility for calculating acceleration variances. There are though, certain problems concerning the calculation of acceleration variances due to uncertainties in the position measurements. Assuming that the position measurements can be split up in the actual particle positions and an uncorrelated noise term with variance σ_i^2, on can show that the difference between the measured and the actual acceleration variance can be expressed as [11]

$$\langle \tilde{a}_i^2 \rangle = \langle a_i^2 \rangle + \frac{6\sigma_i^2}{\Delta t^4} \tag{1}$$

where $\tilde{a}_i$ is the i coordinate of the estimated acceleration, σ_i^2 is the variance in the *noise* on the measurement of the i coordinate of the position measurements, and Δt is the period between acquired images (40 ms). We do not have direct means to separate the variance in the particle coordinates in noise and actual particle positions, but it can be done indirectly.

The first predictions of the variance of particle accelerations in a turbulent flow were made by Heisenberg and Yaglom [19, 20]:

$$\langle a_i^2 \rangle = \frac{a_0 \epsilon^{\frac{3}{2}}}{\nu^{\frac{1}{2}}} \tag{2}$$

where a_0 was predicted to be a universal constant.

Using this prediction and the equation 1, we can use a least squares fit, to estimate a_0 and σ_i. Figure 2 shows our experimental data corrected using $\sigma_i = 0.030$ mm (somewhat larger than the value predicted in [21]) together with the Heisenberg-Yaglom acceleration variance corresponding to $a_0 = 3.3$. The value of a_0 depends on R_λ [1], but we do not have sufficient variations in R_λ to investigate this. When the correlation time, τ_η, for the signal is close to the duration used to estimate accelerations, it is most likely underestimated.

ACCELERATION AUTO-CORRELATION FUNCTIONS

We have calculated coordinate-wise Lagrangian auto-correlation functions of the particle accelerations:

$$R_i(\tau) = \langle a_i(t+\tau) \cdot a_i(t) \rangle \tag{3}$$

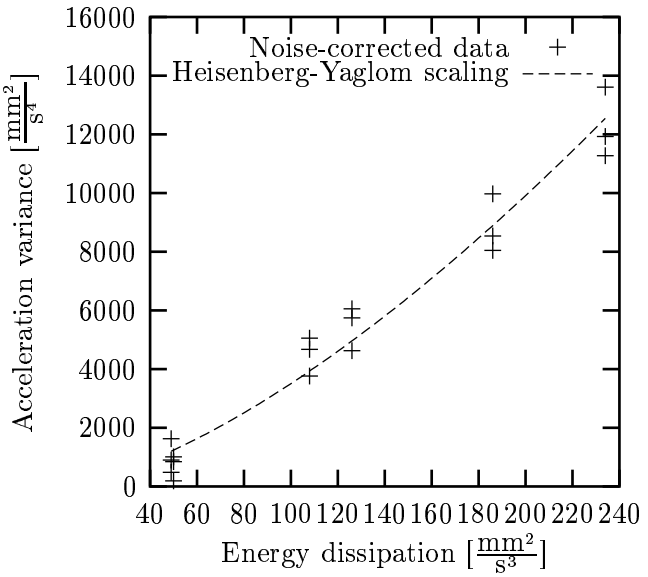

Figure 2: Acceleration variances viewed as functions of the energy dissipation. The data are corrected for an estimated noise in the position measurements.

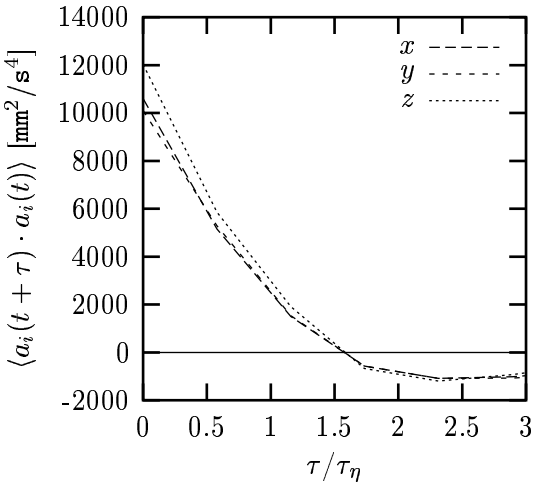

Figure 3: Lagrangian auto-correlation functions for respectively the x, y and z coordinates of the acceleration in run 21.

An example of the result is presented in figure 3. Qualitatively this measured acceleration auto-correlation function has the same shape as the ones from the computer simulations presented in [1]. Assuming stationarity of the Lagrangian velocity, the integral of $R_i(\tau)$ is zero. According to [1], these functions should be zero at $\tau_{zero}/\tau_\eta = 2.2$. Our measurements

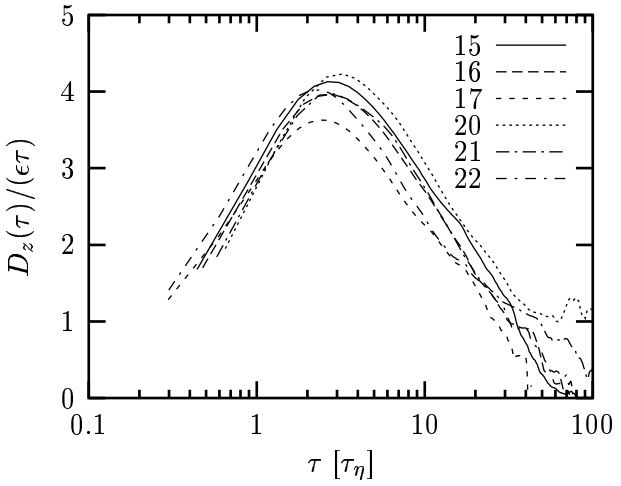

Figure 4: Lagrangian velocity structure functions. The labels refer to the run numbers of the experiment.

of consistently result in smaller values, between 1.4 and 1.8. A correction equivalent to equation 1 may be applied to $R_i(\tau)$ [11]. However this does not alter the zero crossing times significantly.

The discrepancy between numerical simulations and experimental data could to some extent simply reflect that the Kolmogorov constant is not well determined. However, the relatively small differences between the results based on the von Kármán spectrum and on $\langle \delta\vec{a} \cdot \delta\vec{v} \rangle$ indicates that the dissipation is well determined. Until a thorough investigation of how differences in the forcing of computer simulated as well as real flows influences the zero-crossing time of the Lagrangian acceleration auto-correlation functions, one should be careful about using τ_{zero} for estimating the energy dissipation.

VELOCITY STRUCTURE FUNCTIONS

Lagrangian second order velocity structure functions are defined as

$$D_i(\tau) = \langle (v_i(t+\tau) - v_i(t))^2 \rangle, \; i \in \{x, y, z\} \tag{4}$$

In figure 4 we show a collection of second order Lagrangian velocity structure functions normalized with $\epsilon\tau$.

In his paper on Reynolds number effects in Lagrangian stochastic models of turbulent dis-

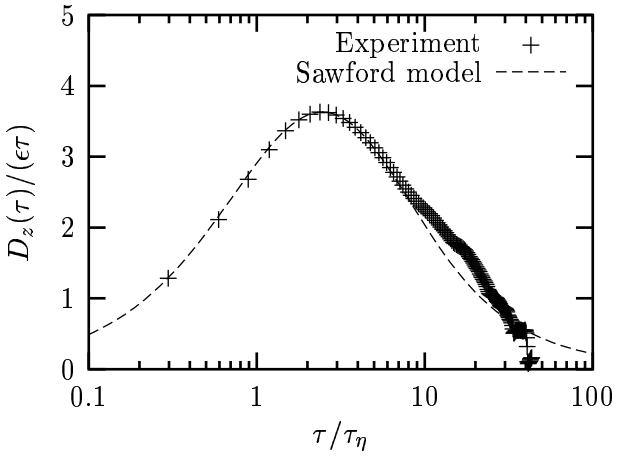

Figure 5: Lagrangian velocity structure function. Run 17 and a Sawford model fitted to the experimental data ($T_0 = 0.081$ s, $T_\infty = 0.466$ s).

persion [2], Sawford uses a refined Langevin model to derive an expression for the normalised Lagrangian velocity correlation function:

$$\rho(\tau) = \frac{T_\infty(1 - e^{-\tau/T_\infty}) - T_0(1 - e^{-\tau/T_0})}{T_\infty - T_0} \tag{5}$$

where T_0 and T_∞ are two time constants obeying the relation $T_0 + T_\infty = T_L$. This can be used to model the second order Lagrangian velocity structure function $D_L(\tau) = 2\sigma^2(1 - \rho(\tau))$, where σ is the velocity standard deviation. Except for large time-lags, τ, where we only have a small number of data points and thus limited statistical significance, this model fits our measurements quite well. This can, for run 17, be seen in figure 5, which shows the experimental curve from figure 4 together with Sawford's model fitted to the experimental data.

It is generally believed that Lagrangian velocity structure functions at sufficiently high Reynolds numbers should in a range of time differences show a power law behavior similar to that we see for Eulerian velocity structure functions. The second order Lagrangian velocity structure functions should in this range take the form $D_i(\tau) = C_0\epsilon\tau$, where C_0 is a universal constant. If this is true, then the maximum of the measured second order Lagrangian velocity structure functions should converge to this constant for large Reynolds numbers. It is clear from figure 4 that we are far from the Reynolds numbers needed to reach the power law regime.

The scaling range for 2nd order Lagrangian structure functions is much smaller than that

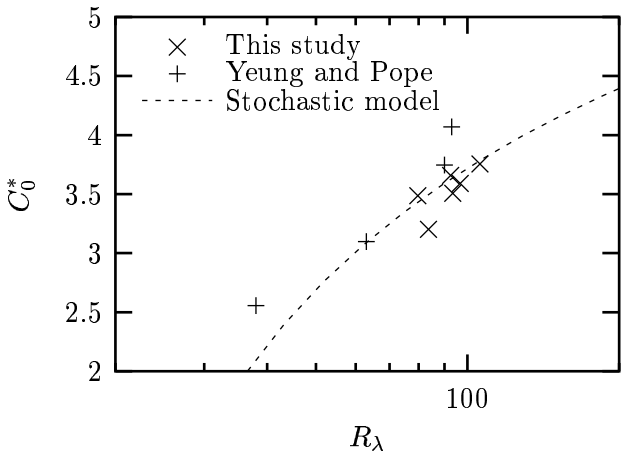

Figure 6: The top values of Lagrangian velocity structure functions (averaged over the three velocity components) as shown in figure 4 (×) and of the ones shown in Sawford's and Pope's papers (+). The dashed line is a numerical solution based on Sawford's stochastic model.

of 2nd order Eulerian structure functions. This means that it is in general comparatively difficult to use the actual power-law which the structure functions approach for increasing Reynolds numbers, for Lagrangian data.

In order to work around this problem Sawford has constructed a stochastic model for Lagrangian velocity structure functions [2]. In his paper on the model he fixes the free parameters of the model using results from direct numerical simulations of the Navier-Stokes equations. In figure 6 we compare a numerical solution for $C_0^*(R_\lambda)$ with our experimental results and with simulations by Yeung and Pope.

CONCLUSION

In conclusion, using a 3D particle tracking experiment, we have estimated the Heisenberg-Yaglom constant, a_0, to 3.3 at $R_\lambda \approx 100$, we have demonstrated that the Kolmogorov scaled zero-crossing time of the Lagrangian acceleration correlation function, τ_{zero}/τ_η, does not appear to be a universal constant, and finally we have shown data which support Sawford's stochastic model for Lagrangian velocity structure functions.

We are grateful to Morten Sparre Andersen for comments and discussions and to The Danish Research Academy and The Danish Technical Research Council (STVF-9601244 and

26-01-0087) for financial support.

---

* Electronic address: sparre@nbi.dk; URL: http://www.nbi.dk/~sparre/

† Risø National Laboratory, P.O. 49, DK-4000 Roskilde, Denmark

[1] P. K. Yeung and S. B. Pope, Journal of Fluid Mechanics **207**, 531 (1989).

[2] B. L. Sawford, Physics of Fluids A **3**, 1577 (1991).

[3] L. F. Richardson, Proc. R. Soc. Lond. A **101**, 709 (1926).

[4] A. N. Kolmogorov, Dokl. Akad. Nauk SSSR **30;4**, 3201 (1941).

[5] G. I. Taylor, Proc. London Math. Soc. **20**, 196 (1921).

[6] P. K. Yeung, Journal of Fluid Mechanics **427**, 241 (2001).

[7] S. B. Pope, Annu. Rev. Fluid Mech. **26**, 23 (1994).

[8] R. E. Davis, Annu. Rev. Fluid Mech. **23**, 43 (1991).

[9] G. A. Voth, K. Satyanarayan, and E. Bodenschatz, Physics of Fluids **10; 9**, 2268 (1998).

[10] G. Boffetta, A. Celani, A. Crisanti, and A. Vulpiani, Europhysics Letters **46;2**, 177 (1999).

[11] J. Mann, S. Ott, and J. S. Andersen, *Experimental Study of Relative, Turbulent Diffusion* (Risø National Laboratory, P.O. Box 49, DK-4000 Roskilde, Denmark, 1999), ISBN 87-550-2370-3, URL http://www.risoe.dk/rispubl/VEA/ris-r-1036.htm.

[12] S. Ott and J. Mann, J. Fluid Mech. **422**, 207 (2000).

[13] A. L. Porta, G. A. Voth, A. M. Crawford, J. Alexander, and E. Bodenschatz, Nature **409;6823**, 1017 (2001).

[14] N. Mordant, P. Metz, O. Michel, and J. Pinton, Physical Review Letters **87** (2001).

[15] M. Virant and T. Dracos, Meas. Sci. Tecnol. **8**, 1529 (1997).

[16] T. von Kármán, Proceedings of the National Academy of Sciences **34**, 530 (1948).

[17] A. S. Monin and A. M. Yaglom, *Statistical Fluid Mechanics*, vol. 2 (The MIT Press, 1975).

[18] J. R. Chasnov, Phys. Fluids A **3;1**, 188 (1991).

[19] Heisenberg, Zschr. f. Phys. **124**, 628 (1948).

[20] A. M. Yaglom, C. R. Akad. URSS **67;5**, 795 (1949).

[21] M. Marxen, P. E. Sullivan, M. R. Loewen, and B. Jahne, Exp. in Fluids **29;2**, 145 (2000).

[22] *Styrocell* from Shell Chemicals.